

On the dissipative effects in the electron transport through conducting polymer nanofibers

Natalya A. Zimbovskaya

*Department of Physics and Electronics, University of Puerto Rico at Humacao, Humacao, PR 00791,
and Department of Physics and Astronomy, University of Pennsylvania, PA 19104-6323, USA*

(Dated: December 2, 2024)

Here, we study the effects of stochastic nuclear motions on the electron transport in doped polymer fibers assuming the conducting state of the material. We treat conducting polymers as granular metals and apply the quantum theory of conduction in mesoscopic systems to describe the electron transport between the metalliclike granules. To analyze the effects of nuclear motions we mimic them by the phonon bath, and we include the electron-phonon interactions in consideration. Our results show that the phonon bath plays a crucial part in the intergrain electron transport at moderately low and room temperatures suppressing the original intermediate state for the resonance electron tunneling, and producing new states which support the electron transport.

PACS numbers: 72.15.Gd,71.18.+y

Currently, electron transport in conducting polymer nanofibers is a subject of intense interest because they are expected to be used in building up nanoelectronic devices. Doped polyacetylen or polyaniline-polyethylene oxide fibers as well as polypyrrole nanotubes could behave as conductors, and their conductivity significantly increases upon doping. Charge transport mechanisms in the conducting polymers were intensively studied starting from the very discovery of these materials [1, 2].

It is known that chemically doped conducting polymers are very inhomogeneous. In some regions polymer chains are disorderly arranged forming an amorphous poorly conducting substance. In other places the chains are ordered and densely packed [3, 4]. The corresponding regions behave as metalliclike grains embedded in a disordered environment. The key point in studies of the electron transport in conducting polymers is to elucidate the nature and physical mechanism of the intergrain transport. Prigodin and Epstein suggest that the intergrain transport mostly occurs due to the electron tunneling between the grains through intermediate resonance states on polymer chains connecting them. This approach was employed to build up the theory of electron transport in polyaniline based nanofibers [5] providing good agreement with the previous transport experiments [6].

An important issue that arises in the analysis of the intergrain electron transport is the influence of nuclear motions in the medium between the grains. The similar issue was analyzed while developing the theory of the conduction through macromolecules. It was shown that the environment acts as a source of incoherence for the tunneling electron [7, 8, 9, 10]. Also, it can give rise to some extra electron states [11, 12]. In the previous works [5, 13] the effect of stochastic nuclear motions in the environment was discussed within the model based on the scattering matrix formalism [14, 15]. Here, we employ another approach which gives means to explicitly describe the effect of environment induced electronic states in the

electron transmission and the electric current in polymer fibers.

Assuming the electron tunneling through the intermediate state to be the predominant mechanism for the intergrain transport, we see a similarity in electron transport mechanisms in conducting polymers and those in molecules connecting metal leads. In the case of polymers the metalliclike domains take on part of the leads, and the molecular bridge in between is reduced to a single intermediate site. To mimic the effects of the environment we assume that the side chain is attached to the bridge, and this chain is affected by a phonon bath including a large amount of harmonic oscillations. This model resembles those used to analyze electron transport through macromolecules [8, 10, 16]. The side chain is introduced to the model to screen the resonance state making it more stable against the effect of the phonon bath. As in the previous papers [10, 16] we assume that electrons cannot hop along the side chain, so it may be reduced to a single site attached to the resonance site (the bridge).

The effective Hamiltonian for the bridge within the adopted model takes on the form:

$$H_{eff} = H + H_L + H_R. \quad (1)$$

Here, $H_{L,R}$ are self-energy terms describing the coupling of the left (L) and right (R) grain to the bridge, and the Hamiltonian H may be presented as follows:

$$H = H_b + H_c + H_{b-c} \quad (2)$$

where $H_b = \epsilon b^+ b$ corresponds to the bridge site, H_c is the Hamiltonian of the side chain, and H_{b-c} describes the interaction between them. The terms H_c and H_{b-c} are modified due to the coupling of the side chain to the bath. Keeping only one site in the side chain we have:

$$H_c = (\tilde{\epsilon} - \delta) c^+ c, \quad (3)$$

$$H_{b-c} = -w\chi(b^+ c + h.c.). \quad (4)$$

Here, $\epsilon, \tilde{\epsilon}$ are the on-site energies and w is the hopping integral between the bridge site and the attached side site, respectively. The quantities δ and χ are given by [10]:

$$\delta = \sum_{\alpha} \frac{\lambda_{\alpha}^2}{\Omega_{\alpha}}, \quad \chi = \exp \left[\sum_{\alpha} \frac{\lambda_{\alpha}}{\Omega_{\alpha}} (B_{\alpha} - B_{\alpha}^+) \right] \quad (5)$$

where Ω_{α} are the frequencies of the phonons belonging to the bath, λ_{α} denote the electron-phonon coupling strengths, and B_{α}^+, B_{α} are the phonon operators of creation and annihilation.

The lowest order in the Fourier transform for the Green's function associated with the Hamiltonian (1) reads:

$$G^{-1}(E) = E - \epsilon - \Sigma_L(E) - \Sigma_R(E) - w^2 P(E). \quad (6)$$

The first four terms in this expression represent the inverse Green's function for the resonance site coupled to the two grains where $\Sigma_{L,R}(E)$ are complex self-energy functions. The last term represents the effect of the environment and has the form [10]:

$$P(E) = -i \int_0^{\infty} dt \exp[i t (E - \tilde{\epsilon} + \delta + i 0^+)] \times \{(1-f) \exp[-F(t)] + f \exp[-F(-t)]\} \quad (7)$$

with $\exp[-F(t)]$ being a dynamic bath correlation function, and f taking on values 1 and 0 when the attached site is occupied and empty, respectively.

Characterizing the phonon bath with a continuous spectral density $J(\omega)$ given by [17]:

$$J(\omega) = J_0 \left(\frac{\omega}{\omega_c} \right) \exp \left[-\frac{\omega}{\omega_c} \right] \quad (8)$$

one may write out the following expressions for the functions $F(t)$ and δ :

$$F(t) = \int_0^{\infty} \frac{d\omega}{\omega^2} J(\omega) \left[1 - e^{-i\omega t} + 2 \frac{1 - \cos(\omega t)}{\exp(\omega/\theta) - 1} \right], \quad (9)$$

$$\delta = \int_0^{\infty} \frac{d\omega}{\omega} J(\omega) = J_0 \quad (10)$$

where θ is the temperature expressed in the units of energy.

After some calculations, the function $F(t)$ could be presented in the form:

$$F(t) = \frac{J_0}{\omega_c} \left\{ \frac{1}{2} \ln[1 + (\omega_c t)^2] + i \arctan(\omega_c t) + K(t) \right\} \quad (11)$$

where

$$K(t) = \theta^2 t^2 \zeta \left(2; \frac{\theta}{\omega_c} + 1 \right) \equiv \theta^2 t^2 \sum_{n=1}^{\infty} \frac{1}{(n + \theta/\omega_c)^2}. \quad (12)$$

Here, $\zeta(2; \theta/\omega_c + 1)$ is the Riemann ζ function [18]. The asymptotic expression for $K(t)$ depends on the relation between two parameters, namely, the temperature θ and the cut-off frequency ω_c characterizing the thermal relaxation rate of the phonon bath. Assuming $\theta \gg \omega_c$ and estimating the sum of the series in Eq. (12) and we get:

$$K(t) \approx \frac{\theta}{\omega_c} (\omega_c t)^2. \quad (13)$$

In the opposite limit $\omega_c \gg \theta$ we obtain:

$$K(t) \approx \frac{\pi^2}{6} (\theta t)^2 \quad (14)$$

Also, we may roughly estimate $K(t)$ within the intermediate range when. Taking $\theta \approx \omega_c$ we arrive at the approximation $K(t) \approx a^2 (\theta t)^2$ where a^2 is a dimensionless constant of the order of unity. Substituting the obtained asymptotics for the function $F(t)$ into Eq. (7) we see that the main contribution to the integral comes from the short times region ($\omega_c t \ll 1$). Therefore in calculations of $P(E)$ we may expand $\Phi(t)$ in series in powers of $\omega_c t$ keeping two first terms in the expansion. At $\theta \gg \omega_c$ we arrive at the result:

$$P(E) = -\frac{i}{2} \sqrt{\frac{\pi}{J_0 \theta}} \exp \left[-\frac{(E - \tilde{\epsilon})^2}{4 J_0 \theta} \right] \left\{ 1 + \Phi \left[\frac{i(E - \tilde{\epsilon})}{2\sqrt{J_0 \theta}} \right] \right\} \quad (15)$$

where $\Phi(z)$ is the probability integral. When both ω_c and θ have the same order of magnitude the expression for $P(E)$ still holds the form (15). At $\theta \ll \omega_c$, the temperature θ in the expression (15) is to be replaced by ω_c . We remark that under the assumption $\theta \gg \omega_c$ the function $P(E)$ does not depend on the cut-off frequency ω_c , whereas at $\omega_c \gg \theta$ it does not depend on temperature. As shown in the Fig. 1, the imaginary part of $P(E)$ exhibits a dip around $E = \tilde{\epsilon}$ and the width of the latter is determined by the product of the temperature θ (or ω_c) and the constant J_0 characterizing the strength of the electron-phonon interaction. When either factor increases, the dip becomes broader and its magnitude reduces.

The presence of $P(E)$ gives rise to very significant changes in the behavior of the Green's function given by the Eq. (6). Using the flat band approximation for the self-energy corrections $\Sigma_{L,R}$, namely: $\Sigma_{L,R} = -i \Delta_{L,R}$ where $\Delta_{L,R}$ are constants of the dimensions of energy, and neglecting for a moment all imaginary terms in the Eq. (6), we find that two extra poles of the Green's function emerge due to the environment. When the phonon bath is detached ($J_0 = 0$) the separation between the poles is determined with the hopping integral w . Due to the electron coupling to the phonons the positions of the poles become shifted. Assuming $\epsilon = \tilde{\epsilon} = 0$ and $\theta \gg \omega_c$ we get:

$$E = \pm 2 \sqrt{J_0 \theta | \ln(2 J_0 \theta / w^2) |} \quad (16)$$

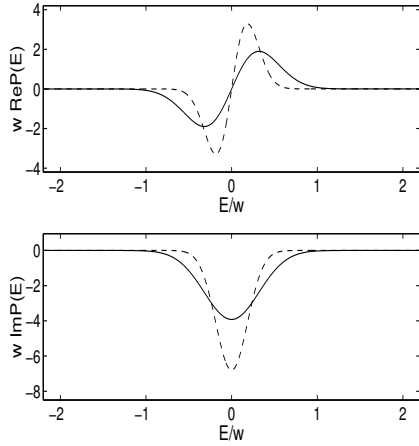


FIG. 1: Energy dependence of the real (top panel) and imaginary (bottom panel) parts of $P(E)$. The curves are plotted assuming $J_0 = 20\text{meV}$, $w = 100\text{meV}$, $\tilde{\epsilon} = 0$, $T = 100K$ (dash lines), and $T = 300K$ (solid lines) at $\theta \gg \omega_c$.

Again, in this expression θ is to be replaced by ω_c when $\omega_c \gg \theta$. The poles correspond to extra electron states which occur due to the electron coupling to the environment. These new states are revealed in the structure of the electron transmission $T(E)$ which reads [19]:

$$T(E) = 4\Delta_L\Delta_R|G(E)|^2. \quad (17)$$

The structure of $T(E)$ is shown in the Fig. 2. Two peaks in the transmission are associated with the environment induced electronic states. Their positions and heights depend on the temperature (or ω_c), J_0 , and w . The important feature in the electron transmission is the absence of the peak associated with the resonance state between the grains (the bridge site) itself. This happens due to the strong suppression of the latter by the effects of the environment. Technically, this peak is damped for it is located at $E = 0$ where the imaginary part of $P(E)$ reaches its maximum in magnitude. So, the effects of the environment may lead to the damping of the original resonance state for the electron tunneling between the metallic islands in the polymer fiber. Instead, two environment induced states emerge to serve as intermediate states for the electron transport. Similar effects were recently investigated in the electron transport through DNA macromolecules [10], and it was shown that low biased current-voltage characteristics may be noticeably changed due to the occurrence of the phonon bath induced electron states. Due to some particular features of conducting polymers, these effects may be revealed in polymer nanofiber current-voltage curves at significantly higher bias voltage, as discussed below.

Realistic polymer nanofibers have diameters within the range $20 \div 100\text{ nm}$, and lengths of the order of a few microns. This is much greater than the typical size of both

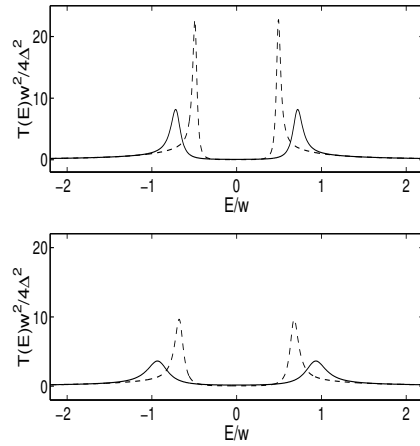


FIG. 2: The renormalized electron transmission function vs energy. The curves are plotted for $\epsilon = \tilde{\epsilon} = 0$, $w = 100\text{meV}$, $T = 100K$ (dash lines) and $T = 300K$ (solid lines). The constant J_0 equals 20meV (top panel) and 50meV (bottom panel).

metalliclike grains and intergrain separations which take on values $\sim 5 \div 10\text{ nm}$ [20]. Therefore, we may treat a nanofiber as a set of parallel working channels, any single channel being a sequence of grains connected with the resonance polymeric chains. The net current in the fiber is the sum of currents flowing in these channels, and the voltage V applied across the whole fiber is distributed among sequential pairs of grains along a single channel. So, the voltage ΔV applied across two adjacent grains could be estimated as $\Delta V \sim VL/L_0$ where L is the average separation between the grains, and L_0 is the fiber length. The ratio $\Delta V/V$ may take on values of the order of $10^{-1} \div 10^{-2}$. Experiments on the electrical characterization of the polymer fibers are usually carried out at moderately high temperatures ($T \div 300K$), so it seems likely that $\theta > \omega_c$. Assuming that $w \sim 100\text{meV}$, and $J_0 \sim 20 \div 50\text{meV}$ we estimate the separation between the environment induced peaks in the electron transmission as $120 \div 170\text{meV}$ (see Fig. 2). This estimate is close to $e\Delta V$ when V takes on values up to $2 \div 3$ volts. So, the environment induced peaks in the electron transmission determine the shape of the current-voltage curves even at reasonably high values of the bias voltage applied across the fiber.

In calculations of the current we employ the formula [19]:

$$I = \frac{2en}{h} \int_{-\infty}^{\infty} dE T(E) [f_1(E) - f_2(E)]. \quad (18)$$

Here, n is the number of the working channels in the fiber, $f_{1,2}(E)$ are Fermi functions taken with the different contact chemical potentials $\mu_{1,2}$ for the grains. The chemical potentials differ due to the applied bias voltage

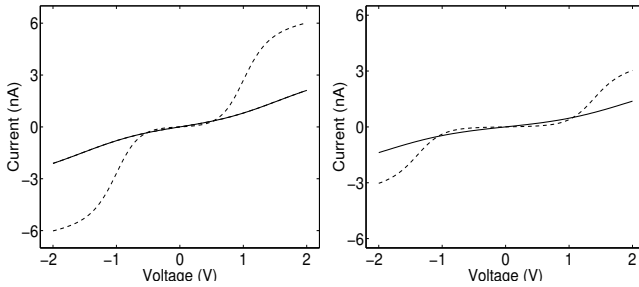


FIG. 3: The current-voltage characteristics plotted for $n = 10$, $\Delta_L = \Delta_R = 0.5\text{meV}$, $\eta = 1/2$, $w = 100\text{meV}$, $J_0 = 20\text{meV}$ (left panel), and $J_0 = 50\text{meV}$ (right panel) at $T = 100\text{K}$ (dash lines) and $T = 300\text{K}$ (solid lines).

ΔV :

$$\mu_1 = E_F + (1 - \eta)e\Delta V; \quad \mu_2 = E_F - \eta e\Delta V. \quad (19)$$

The parameter η characterizes how the voltage ΔV is divided between the grains; E_F is the equilibrium Fermi energy of the system including the pair of grains and the resonance site in between, and $T(E)$ is the electron transmission function given by Eq. (17).

The resulting current-voltage characteristics are shown in the Fig. 3. The current takes on low values ($\sim 1\text{nA}$) because the coupling of the grains to the intermediate state is weak due to comparatively large distances between the grains [2]. Consequently, $\Delta_{L,R}$ take on values much smaller than those typical for electron transport through molecules placed between metal leads. The $I-V$ curves exhibit a nonlinear shape even at room temperature despite the fact that the original state for the resonance tunneling is completely washed out. This occurs for the intergrain transport is supported by new phonon induced electron states. In this work we did not take a task of providing a quantitative agreement between the theory and experimental results obtained on conducting polymer fibers. However, in general, our calculated $I-V$ curves agree with the reported experiments [7].

It is worthwhile to briefly discuss the temperature dependence of the electric current which follows from the present results. At moderately low temperatures $T \sim 100\text{K}$, the latter is mostly determined by the behavior of the electron transmission function. Omitting small corrections $\Delta_{L,R}$ in the Eq. (6) and using the expression (15) for $P(E)$ we may conclude that the transmission (and the current) approximately follows the Arrhenius law being proportional to $\exp(-T_0/T)$ where T_0 is the constant of the dimensions of temperature. However, at higher temperatures ($T \sim 300\text{K}$) the temperature dependence of the current is different and more complicated.

Finally, the present analysis shows that the stochastic nuclear motions in the medium between the grains (especially those in the resonance chain) take a crucial part in the electron transport in the conducting polymers at moderately low and room temperatures. Due to their influence the original intermediate state for the resonance tunneling becomes completely suppressed but new environments induced states appear providing the electron transport through the polymer nanofibers.

Acknowledgments: Author thank M. L. Klein and A. T. Johnson Jr. for useful discussions and G. M. Zimbovskiy for help with the manuscript. This work was supported by NSF Advance program SBE-0123654 and NSF-PREM 0353730.

- [1] A. G. MacDiarmid, Rev. Mod. Phys. **73**, 701 (2001).
- [2] See e.g. V. N. Prigodin and A. J. Epstein, Synth. Met. **125**, 43 (2002) and references therein.
- [3] J. Joo, Z. Oblakowski, G. Du, J. P. Ponget, E. J. Oh, J. M. Wiessinger, Y. Min, A. G. MacDiarmid, and A. J. Epstein, Phys. Rev. B **49**, 2977 (1994).
- [4] J. P. Ponget, Z. Oblakowski, Y. Nogami, P. A. Albony, M. Laridjani, E. J. Oh, Y. Min, A. J. MacDiarmid, J. Tsukamoto, T. Ishiguro, and A. J. Epstein, Synth. Met. **65**, 131 (1994).
- [5] N. A. Zimbovskaya, A. T. Johnson Jr., and N. J. Pinto, Phys. Rev. B **72**, 024213 (2005).
- [6] Yangxin Zhou, M. Freitag, J. Hone, C. Stali, A. T. Johnson Jr., N. J. Pinto, and A. G. MacDiarmid, Appl. Phys. Lett. **83**, 3800 (2003).
- [7] A. Nitzan, Ann. Rev. Phys. Chem. **52**, 681 (2001).
- [8] X. Q. Li and Y. Yan, Appl. Phys. Lett. **81**, 925 (2001).
- [9] M. Galperin, A. Ratner, and A. Nitzan, J. Chem. Phys. **121**, 11965 (2004).
- [10] R. Gutierrez, S. Mandal, and G. Cuniberti, Phys. Rev. B **71**, 235116 (2005).
- [11] R. G. Endres, D. L. Cox, and R. R. P. Singh, Rev. Mod. Phys. **76**, 195 (2004).
- [12] F. L. Gervasio, P. Carloni, and M. Partinello, Phys. Rev. Lett. **89**, 108102 (2002).
- [13] N. A. Zimbovskaya, J. Chem. Phys. **123**, 114708 (2005).
- [14] M. Buttiker, Phys. Rev. B **33**, 3020 (1986).
- [15] X. Q. Li and Y. J. Yan, J. Chem. Phys. **115**, 4169 (2001).
- [16] G. Cuniberti, L. Craco, D. Porath, and C. Dekker, Phys. Rev. B **65**, 241314(R) (2002).
- [17] G. D. Mahan, *Many-Particle Physics* (Plenum, New York, 2000).
- [18] I. S. Gradshteyn and I. M. Ryzhik, *Tables of Integrals, Series and Products* (Academic, New York, 2000).
- [19] S. Datta, *Electronic Transport in Mesoscopic Systems* (Cambridge University Press, Cambridge, England, 1995).
- [20] See e.g. R. Pelster, G. Nimtz, and B. Wessling, Phys. Rev. B **49**, 12718 (1994).